Trajectory Optimization with Risk Minimization for Military Aircraft

John L. Vian and John R. Moore
Boeing Military Airplane Company, Wichita, Kansas

Methods of time-controlled optimal flight-trajectory generation are developed that include the effects of risk from a threat environment. Lateral and vertical algorithms are developed for military jet aircraft with the intent of near real-time application. Simple analytic functions are used for threat models, as the focus of this paper is on general problem formulation and not detailed solutions for specific threats. A constant altitude, lateral flight-trajectory generation method is developed that optimizes with respect to time, fuel, final position, and risk exposure. Existing vertical plane trajectory generation methods that use standard direct operating costs of time and fuel are modified to include the effect of risks. Singular perturbation methods are used to obtain reduced-order airplane models that allow static rather than dynamic optimization. Pontryagin's Minimum Principle is used with a Fibonacci search method to minimize the cost functional. Formulation and numerical results are presented for both the horizontal and vertical plane problems.

Introduction

IN the 1970's, rising fuel prices and improved microprocessor capability made consideration of onboard flight-path optimization appealing as a way to reduce operating costs. More recently, increased air traffic and the associated control problems have shifted research emphasis toward four-dimensional trajectory optimization. The four-dimensional problem typically includes a cost of time that allows trajectories to meet required times of destination arrival. The majority of research in this area has been directed toward commercial operations and involves using the energy state approximation for generating vertical flight paths. It has been shown[1-4] that singular perturbation theory (SPT) may be used successfully to reduce the order of this problem. A reduced-order, often static, optimization technique can then be employed that greatly reduces computational burden. In this paper, methods of trajectory generation are developed that expand the basic SPT techniques to address the needs of military operations.

Trajectory generation will be a fundamental requirement for future military aircraft flight management systems. These systems will be required to take advantage of all available information to perform integrated task processing and reduce pilot workload. In addition, the systems should be able to provide updates at any time throughout a mission or at regular time intervals sufficient for threat avoidance. Much of the previous work in trajectory generation for military aircraft[5-7] has concentrated on feasible directions algorithms that use dynamic programming. These methods tend to be computationally intense and, therefore, are not well suited for onboard applications in dynamic threat environments.

An ideal flight trajectory for military operations meets the mission requirements within the constraints of the aircraft limitations while minimizing exposure to threats. Several levels of information are used in the selection of such a strategic flight path and velocity profile. The trajectory will be a function of mission requirements (time of arrival, point of arrival, etc.), aircraft performance limitations (for example, fuel quantity and thrust limits), and the threat environment. The threat models used in this study do not refer to any specific military scenario. They are simple analytic functions

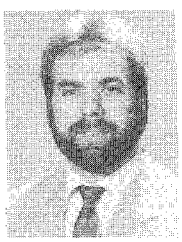

John L. Vian was born in Auburn, Indiana, in 1959. He received a B.S. in mechanical engineering from Purdue University in 1981 and an M.S. in aeronautical engineering from the Wichita State University in 1986, where he is currently pursuing a Ph.D. in engineering. Since 1982, he has been with Boeing Military Airplane Company in Wichita, Kansas, where he is a Senior Specialist Engineer in the Flight Controls Research organization. While at Boeing, he has conducted control system analysis and simulation development on various autonomous flight vehicle programs. He is currently involved with research and development activities related to integrated flight control/flight management systems for military aircraft. Mr. Vian's current research interests are in singular perturbation and the application of stochastic and optimal control to integrated propulsion, flight control, and flight management configurations. He is a licensed Professional Engineer in the State of Kansas and is a member of IEEE and ASME.

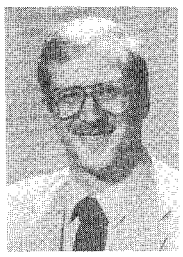

John R. Moore was born in Henderson, Kentucky, in 1959. He was raised in Greensburg, Kentucky, where he was Valedictorian of the 1977 class of Green County High School. In 1982 he earned B.S. degrees in electrical and mechanical engineering from Rose-Hulman Institute of Technology, Terre Haute, Indiana. He also received an M.S. in electrical engineering from the Wichita State University in 1987. Since completing his undergraduate work in 1982, Mr. Moore has been employed by the Boeing Military Airplane Company in Wichita, Kansas. He is currently a Specialist Engineer assigned research and program tasks relating to near-term implementation of four-dimensional trajectory optimization algorithms on military aircraft. Past assignments have included optimal control law development on a variety of research tasks and real-time simulation development to evaluate these concepts. Mr. Moore is a member of Tau Beta Pi and Pi Tau Sigma.

Received June 8, 1987; presented as Paper 87-2523 at the AIAA 1987 Guidance, Navigation, and Control Conference, Monterey, CA, Aug. 17-19, 1987; revision received Jan. 11, 1988.

that characterize the general nature of threats. It is intended to develop and demonstrate methods of optimal trajectory generation using SPT techniques with these general risk models, which would then be updated with high-fidelity models for practical use.

Airplane Model

Aerodynamic and engine data for the airplane model are provided through polynomial curve fits of tabular data given for a jet transport/airlifter class of aircraft. A point mass approximation along with a flat-Earth assumption is made that allows the use of an inertial reference system. The equations of motion are then given by

$$\frac{dx}{dt} = V\cos(\psi)\cos(\gamma) \tag{1}$$

$$\frac{dy}{dt} = V\sin(\psi)\cos(\gamma) \tag{2}$$

$$\frac{dh}{dt} = V\sin(\gamma) \tag{3}$$

$$\frac{dE}{dt} = \frac{V(T-D)}{mg} \tag{4}$$

$$\frac{d\psi}{dt} = \frac{L\sin(\phi)}{mV\cos(\gamma)} \tag{5}$$

$$\frac{d\gamma}{dt} = \frac{L\cos(\phi) - mg\cos(\gamma)}{mV} \tag{6}$$

$$\frac{dm}{dt} = -f \tag{7}$$

where x is downrange position, y cross track position, h altitude, E energy height, ψ heading angle, D drag, T thrust, V velocity, g gravitational constant, γ climb angle, ϕ bank angle, L lift, f fuel flow rate, and m aircraft mass.

Singular Perturbation Application

Singular perturbation techniques[8] depend on identifying distinct time-scale separations that occur in a given system. This allows "slow" and "fast" parts of the system to be solved independently. These individual models are of reduced order and are, therefore, generally easier to solve. The separate solutions are then combined to form a composite approximation to the complete solution. The degree of time-scale separation dictates the degree of error in the composite solution.

For linear systems, determining the time-scaling parameters involves obtaining the eigenstructure of the system to identify its modes. However, in the case of nonlinear systems, such as an airplane model, there is no standard way of determining time-scale separations. In this case, past experience and ad hoc methods must be relied upon in formulating the problem.

Past work has helped in identifying the separation of time scales for transport aircraft in the vertical plane. With sufficiently long cruise legs, it has been shown[3] that energy height E varies on a faster time scale than mass m and range x. A similar analogy can be made for flight in a horizontal plane. If the lateral deviation from a straight-line flight path takes place in a short time compared to the cruise time, then lateral position y can be said to vary on a faster time scale than range x. Figure 1 depicts the fast and slow dynamics of these state variables for the typical long-range mission with a single-threat avoidance maneuver as covered in this study.

Risk Definition

Choosing a flight path and velocity profile to minimize risk and meet mission requirements relies heavily on obtaining, defining, and utilizing all available information about the threat environment. The risk associated with a threat is a function of many variables, and must be defined in such a way that the information can be used to minimize risk exposure. The assumption made in this study is that risk can be quantified in terms of risk index per unit time for any particular location. The simplified threat models in this study assume risk to be a function of position only, as shown below. The cost due to risk is minimized in the optimization process and could be provided to the pilot with every trajectory solution.

Cost of risk:

$$J_r = \int_{t_0}^{t_f} (C_r r)\, dt \tag{8}$$

where C_r = cost of risk factor and r = risk (unit risk/s).

Risk functions:

Radial risk function—

$$r = \frac{1}{d^2} \qquad \text{(unit risk/s)} \tag{9}$$

where d = distance from threat (n. mi.).

Altitude risk function—

$$r = \frac{1}{h^2} \qquad \text{(unit risk/s)} \tag{10}$$

where h = altitude (ft).

Uniform risk function—

$$r = \text{const} \qquad \text{(unit risk/s)} \tag{11}$$

for aircraft in risk area, and $r = 0$ otherwise.

Horizontal Plane Problem

The horizontal plane aircraft motion is modeled using the lateral equations of motion taken from Eqs. (1–7).

$$\frac{dx}{dt} = V\cos(\psi) \tag{12}$$

$$\frac{dy}{dt} = V\sin(\psi) \tag{13}$$

$$\frac{dm}{dt} = -f \tag{14}$$

$$\frac{d\psi}{dt} = \frac{L\sin(\phi)}{mV} \tag{15}$$

$$\frac{dE}{dt} = \frac{V(T-D)}{mg} \tag{16}$$

The lateral trajectory generation problem involves determining the admissible control that satisfies the physical system constraints and also minimizes a performance criterion, or cost function. A cost function is developed that contains terms to penalize time enroute, fuel burn, flight through risk areas, and point of arrival accuracy. This cost function is written as

$$J = \frac{1}{2}\mathbf{x}^T(t_f)S\mathbf{x}(t_f) + \int_{t_0}^{t_f} (C_t + C_f f + C_r r)\, dt \tag{17}$$

where $\mathbf{x}$ is the state vector, S the final state cost matrix, C_t the cost of time, and C_f the cost of fuel.

The cost for final position error is manipulated as follows and included in the integral expression. It, therefore, will be taken into account throughout the optimization procedure.

Let

$$g(t_f) = x^T(t_f)Sx(t_f) = \int_{t_0}^{t_f}\left[\frac{d}{dt}g(t)\right]dt + g(t_0) \tag{18}$$

The last term is dropped from the expression because it is constant and has no effect on the minimization process. The remaining integral term can now be expressed as a combination of a function of x and a function of t by using the chain rule of differentiation as follows:

$$\frac{d}{dt}g(t) = \frac{\partial g(t)}{\partial x}\frac{dx}{dt} + \frac{\partial g(t)}{\partial t}\frac{dt}{dt} = [2Sx(t)]^T\frac{dx}{dt} + 0 \tag{19}$$

Therefore,

$$g(t_f) = \int_{t_0}^{t_f}[2Sx(t)]^T\dot{x}\,dt \tag{20}$$

The cost function may now be written as

$$J = \int_{t_0}^{t_f}\{[Sx(t)]^T\dot{x} + C_t + C_f f + C_r r\}\,dt \tag{21}$$

If S is a diagonal matrix and $y(t_f)$ is the only final state that is penalized, the cost function becomes

$$J = \int_{t_0}^{t_f}(s_y y\dot{y} + C_t + C_f f + C_r r)\,dt \tag{22}$$

Pontryagin's Minimum Principle[9] is used to determine the control input combinations that minimize the cost function. The Hamiltonian used with this method is defined as

$$H = \{\text{cost integrand}\} + \lambda^T\dot{x} \tag{23}$$

The necessary conditions for optimality are given by

$$H^* = \min\{H\}, \qquad \text{in general} \tag{24}$$

$$H^* = 0, \qquad \text{free } t_f\text{, unconstrained} \tag{25}$$

The optimal control that satisfies the preceding necessary conditions can be found using a static optimization procedure if there is only one unknown costate parameter λ. Using the naturally occurring time-scale separations and singular perturbation, the order of the airplane model is reduced as shown below. The lateral equations are written below using the parameters ε and σ to show the separation between fast and slow states. It has been shown[1] that $\varepsilon \simeq 0.08$ for cruise conditions. In addition, σ has been determined to be approximately 0.10 for a 500 n.mi. mission with one risk area as covered in this study.

$$\frac{dx}{dt} = V\cos(\psi) \tag{26}$$

$$\sigma\frac{dy}{dt} = V\sin(\psi) \tag{27}$$

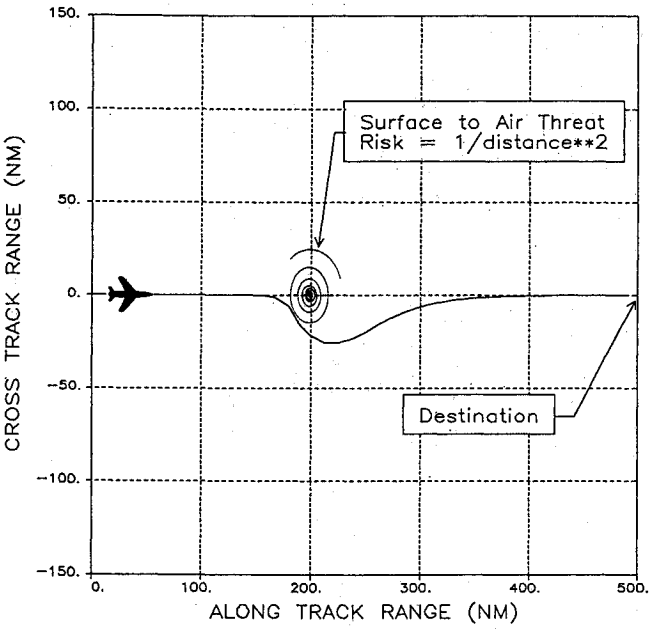

Fig. 2 Ground track for horizontal-plane optimization.

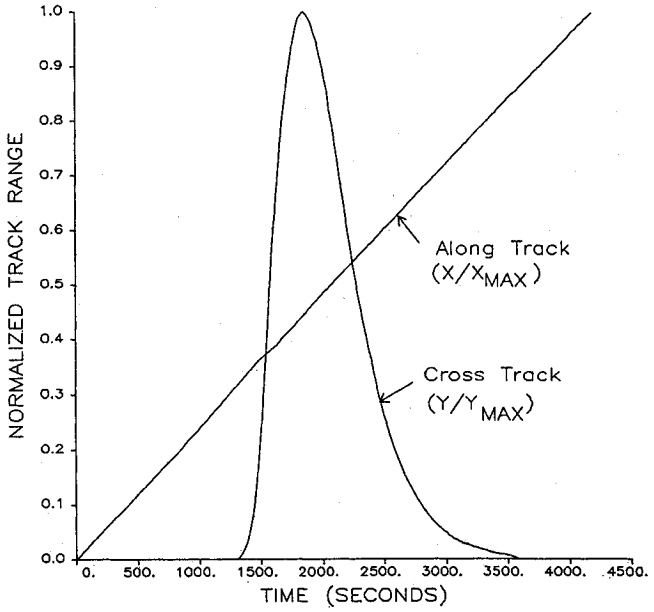

Fig. 1 Along track and cross-track dynamics.

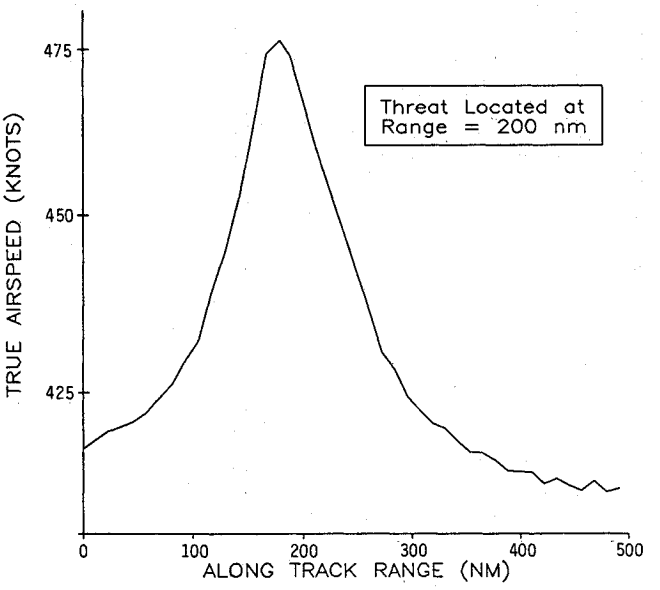

Fig. 3 True airspeed for horizontal-plane optimization.

$$\frac{dm}{dt} = -f \tag{28}$$

$$\varepsilon \frac{dE}{dt} = \frac{V(T-D)}{mg} \tag{29}$$

$$\varepsilon \frac{d\psi}{dt} = \frac{L \sin(\phi)}{mV} \tag{30}$$

The solution to the problem where $\varepsilon = 0.08$ and $\sigma = 0.10$ can be approximated by the composite solution to the singularly perturbed model obtained by letting ε and σ approach zero. The singularly perturbed system is then modeled by the set of state and constraint equations that follow.

$$\frac{dx}{dt} = V \cos(\psi) \tag{31}$$

$$\frac{dm}{dt} = -f \tag{32}$$

$$T = D \tag{33}$$

$$\psi = D \tag{34}$$

$$\phi = 0 \tag{35}$$

The above equations are used to obtain a single outer-type solution for the entire trajectory in the horizontal plane. This near-optimal reduced control results in a performance index that approximates the optimal performance index within $O(\sigma)$.

Using the reduced-order model in Eq. (23), the Hamiltonian becomes

$$H = s_y y\dot{y} + C_t + C_f f + C_r r + \lambda_x \dot{x} + \lambda_m \dot{m} \tag{36}$$

Past work[2] in the vertical plane has determined the value of λ_m to be negligible during cruise portions of flight for transport/airlifter-class aircraft. When λ_m is taken as zero, the minimization of the Hamiltonian can be reduced to a static optimization of the range adjoint variable as written below.

$$-\lambda_x = \min_{V,\psi} \left\{ \frac{s_y y\dot{y} + C_t + C_f f + C_r r}{\dot{x}} \right\} \tag{37}$$

Equation (37) can be minimized by searching over all possible system inputs. If there is not complete time-scale separation, then $\psi \neq 0$ for the true outer solution in the vicinity of the risk. An approximate outer solution is, therefore, obtained by searching both velocity V and heading ψ. A Fibonacci search method is used due to its speed of convergence on unimodal functions. The search uses polynomial curve fits of the tabular performance data to determine the feasibility of the control inputs.

Horizontal Plane Example

A 500 n.mi., 30,000-ft constant-altitude refueling mission is presented as an example. A surface-to-air missile-type threat is positioned directly in the flight path 200 n.mi. into the flight. A radial risk density function, Eq. (9), is used to model the threat. The following cost function parameters are used for this example.

$$C_t = 10.0/\text{s}, \qquad C_r = 3{,}000{,}000/\text{unit risk}$$

$$s_y = 0.061/\text{ft}^2, \qquad C_f = 0.12/\text{lb}$$

The resulting lateral flight path and velocity profile are shown on Figs. 2 and 3. To obtain a different fuel usage, arrival time, or risk assumption, the cost of fuel C_f, cost of time C_t, or the cost of risk C_r would have to be iterated, respectively.

Application Potential

Airlift operations, bombing runs, and aerial refueling are typical missions that have a requirement of near real-time trajectory generation. This task has traditionally been accomplished by preflight mission planning and pilot updates. In complex military environments with multiple dynamic threats and changing mission requirements, the preflight plan becomes obsolete, and the pilot becomes overwhelmed with the amount of available information and the complexity of the calculations required to solve the temporal/spatial problem of trajectory optimization. To demonstrate the application potential of the lateral algorithm, a scenario is set up similar to the first example, only with three pop-up threats and two different required times of arrival (RTA). Figures 4 and 5 show the flight path and velocity profile for the original RTA of 01:11:40 and the updated trajectories for a new RTA of 01:06:40.

Vertical Plane Problem

The vertical plane aircraft motion is modeled using the energy state approximation equations shown below.

$$\frac{dm}{dt} = -f \tag{38}$$

$$\frac{dx}{dt} = V \tag{39}$$

$$\frac{dE}{dt} = \frac{V(T-D)}{mg} \tag{40}$$

The energy height E is related to altitude and velocity by

$$E = h + \frac{V^2}{2g} \tag{41}$$

It is desired to find the admissible control that results in an admissible vertical-plane trajectory from the aircraft initial state at t_0 to a final state at t_f that minimizes the cost functional

$$J = \int_{t_0}^{t_f} (C_t + C_f f + C_r r)\, dt \tag{42}$$

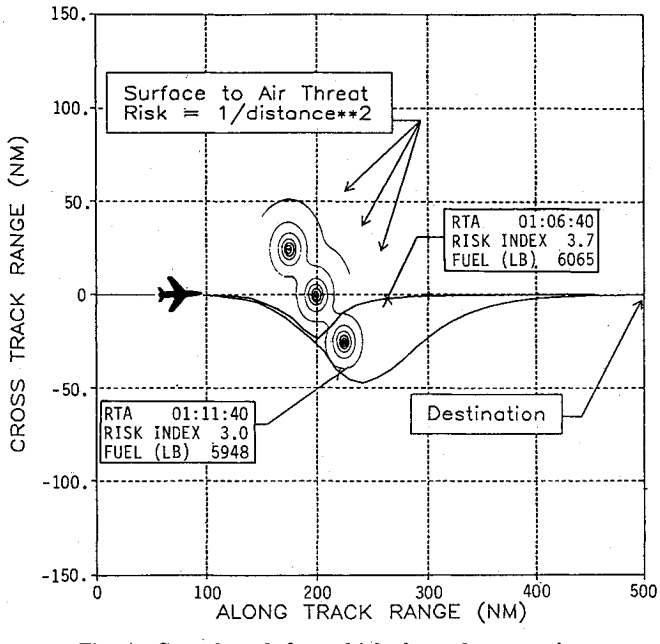

Fig. 4 Ground track for multiple-threat demonstration.

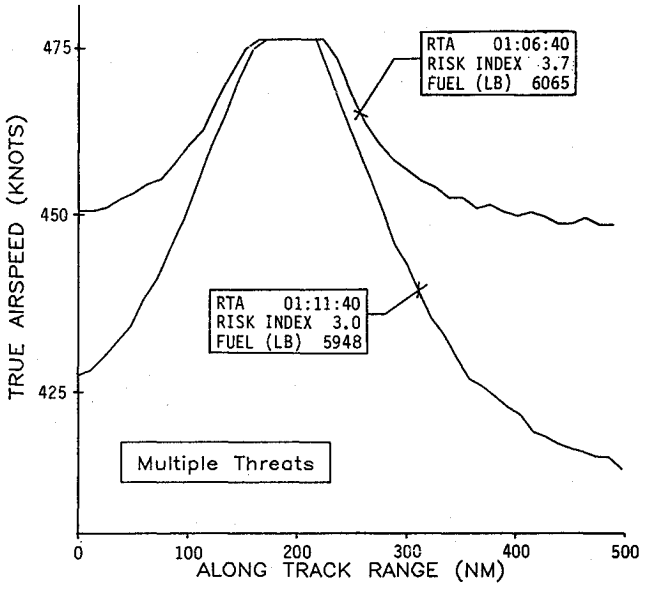

Fig. 5 True airspeed for multiple-threat demonstration.

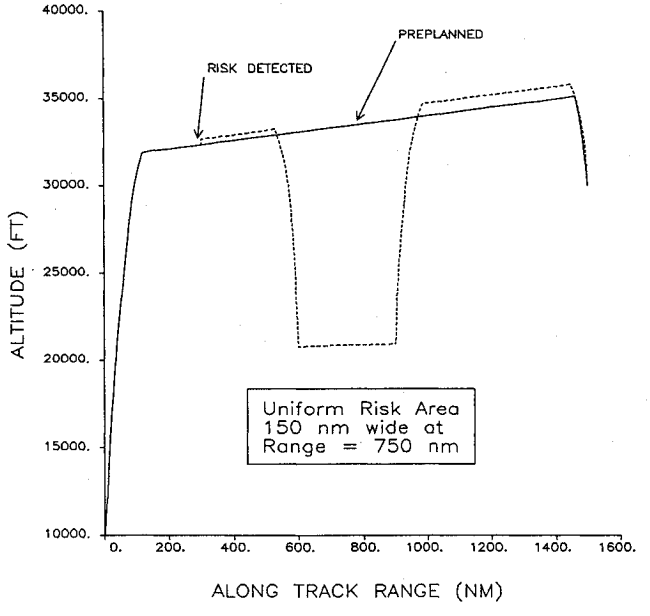

Fig. 6 Altitude profile for vertical-plane optimization.

In general, the final time could be fixed or free. It has been shown[1,2] that if the integrand of Eq. (42) does not explicitly depend on time, then the solution to a fixed arrival time problem can be found by iterating the free arrival time solution with varying costs of time until the actual arrival time is within tolerance to the required arrival time. If the cost of risk C_r in Eq. (16) is set equal to zero, the standard minimum direct operating cost problem[1] results.

Care must be taken to ensure that the singular perturbation assumptions are satisfied. If the range for a mission is so short that the climb and descent overlap with no distinct cruise segment, then the energy height no longer can be considered fast compared to the range. Similarly, the risk density function may cause the aircraft to maneuver in a way that causes energy height to vary on approximately the same time scale as range for a local region in the vicinity of the risk. This will also alter the singularly perturbed structure previously assumed. The vertical plane problem here considers only specific cases where the singular perturbation assumptions for the standard minimum direct operating cost problem[1] are applicable as stated. A sufficient condition is that risk density as a function of range is only allowed to vary stepwise at discrete points that are further apart than the range required for the climb or descent segment. The risk density can otherwise vary continuously as a function of aircraft altitude, speed, and mass without introducing significant error by using the SPT assumptions. Also, for the standard method of iterating the cost of time in a free arrival time problem, the integrand of Eq. (42) and, therefore, the risk density, must not be explicit functions of time.

Outer Solution

Assuming the total range and risk radius are large compared to the climb/descent ranges, Eqs. (38–40) can be rewritten as a set of singularly perturbed equations:

$$\frac{dm}{dt} = -f \tag{43}$$

$$\frac{dx}{dt} = V \tag{44}$$

$$\varepsilon \frac{dE}{dt} = \frac{V(T-D)}{mg} \tag{45}$$

where ε is a small parameter arising from the time-scale separation of energy height E from mass m and range x. The approximate solution to the outer (slow) problem is obtained by applying SPT and letting ε approach zero. This results in a reduced second-order problem and the constraint that thrust equals drag. Using the cost functional, Eq. (16), the Hamiltonian for the outer solution can be written as

$$H_0 = C_t + C_f f + C_r r - \lambda_m f + \lambda_x V \tag{46}$$

The fixed arrival time problem is solved as an iteration of the free arrival problem with an appropriate cost of time in Eq. (46). As stated in Eq. (25), the Hamiltonian for this problem is equal to zero throughout the optimal solution. Again using the results that Burrows[2] obtained, λ_m is assumed to be zero. These conditions can be combined into the following static condition of optimality:

$$\lambda_x = \min_{h,\, V,\, T=D} \left\{ \frac{C_t + C_f f + C_r r}{V} \right\} \tag{47}$$

As mass and range are integrated, the optimal values for λ_x are determined and stored for the inner (fast) solution.

Inner Solution

The outer solution previously outlined results in constant energy segments that are discontinuous at the initial condition, final condition, and risk boundaries. A time-scaled set of equations for the fast variable E is used to match boundary conditions and to transition between energy levels at the risk boundaries.

The time-scale transformation is

$$\tau = (t - t_b)/\varepsilon \tag{48}$$

where t_b is the time at the boundary from the outer solution. As ε approaches zero in the following relationship in the fast boundary layer results

$$\frac{dE}{d\tau} = \frac{V(T-D)}{mg} \tag{49}$$

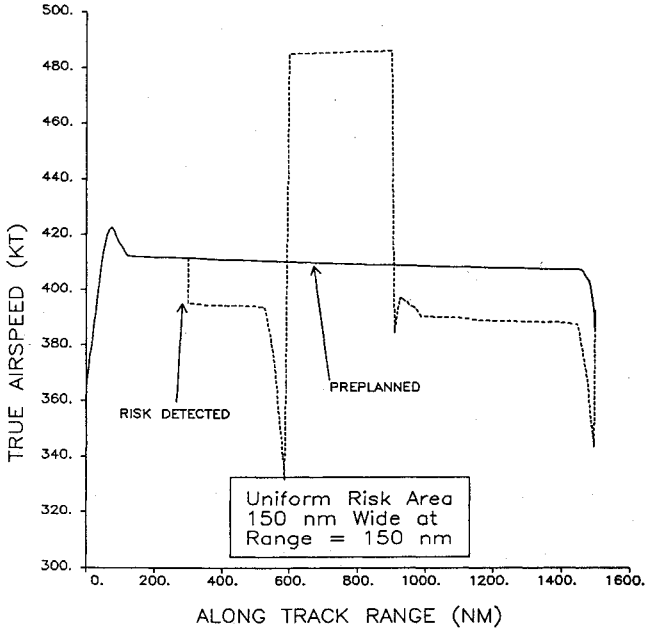

Fig. 7 True airspeed profile for vertical-plane optimization.

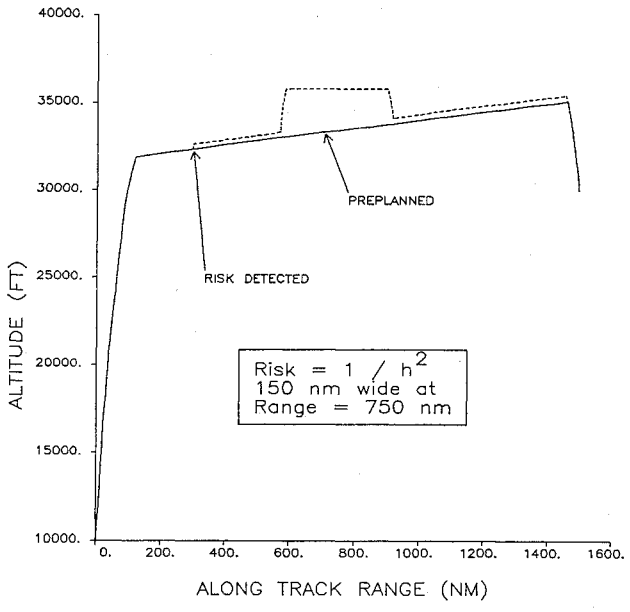

Fig. 8 Altitude profile for vertical-plane optimization.

Recalling the assumption that the mass adjoint vanishes ($\lambda_m = 0$), the Hamiltonian for the inner solution is written as

$$H_i = C_t + C_f f + C_r r + \lambda_{x0} V + \lambda_E \frac{(T-D)V}{mg} \tag{50}$$

where λ_{x0}, the range adjoint from the outer solution, is assumed constant throughout the inner solution. As in the outer solution, the Hamiltonian must be a minimum over all admissible controls and must be equal to zero throughout the optimal trajectory. From these statements, the inner solution condition for optimality is

$$\lambda_E = -\min_{T,V} \left\{ \frac{(C_t + C_f f + C_r r + \lambda_{x0} V)mg}{V(T-D)} \right\} \tag{51}$$

Vertical Plane Example

Numerical results were generated using a mission segment of 1500 n.mi. ending at an aerial rendezvous point. The mission is first planned with final time free and cost of time equal to zero to give the maximum range cruise solution. The time required is recorded and used as a fixed arrival time for the risk minimization solution. At a point 300 n.mi. from departure, a single risk of the form in Eq. (11) is detected. This risk is located 750 n.mi. from the terminal point and has a radius of 150 n.mi. It is assumed that there are no fuel restrictions in the segment. As a result, C_r is allowed to approach infinity (i.e., C_f and C_t effectively go to zero in the areas of nonzero risk). This results in the standard minimum time solution of nonzero risk. The areas of no risk are characterized by the standard minimum direct operating cost problem. Figures 6 and 7 show the altitude and true airspeed profiles for this mission segment. The airspeed away from the risk is lower than preplanned because the arrival time is fixed, and the aircraft proceeds at maximum velocity in the presence of the risk. This maximum velocity takes place at the maximum Mach equivalent airspeed corner, which is at altitudes significantly lower than standard cruise. A significant fuel penalty is paid for the increased speed of transit through the lower altitude area. In this example, a 15% decrease in exposure time (from preplanned profile) requires 60% more fuel burn in the high-risk area. If available fuel is limited, C_r can be iterated until total fuel used is within the constraint.

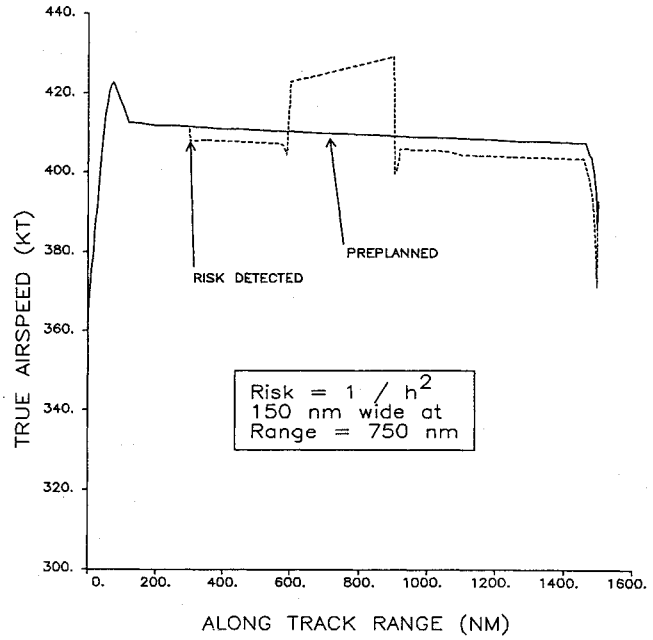

Fig. 9 True airspeed profile for vertical-plane optimization.

The fact that the trajectory is closer to the ground may be a concern if the threat is on the surface. This can be addressed by allowing the risk density function to be a function of altitude, as shown in Eq. (10). The risk density varies continuously with altitude, but only stepwise as a function of horizontal position for reasons discussed earlier. Figures 8 and 9 show the altitude and true airspeed profiles using the altitude-varying risk function.

Conclusions

Current and projected missions for military aircraft will require optimal four-dimensional trajectories to be updated with sufficient frequency to avoid dynamic threats and mission plan updates. The results of this study indicate that

algorithms using time-scale separations are able to meet these requirements. Required computation time using a VAX 11/780 range from 20 to 40 s. The FORTRAN code used for this study was developed to demonstrate feasibility of the proposed algorithms with little regard to execution time. The computation time could be greatly reduced by improving the code structure. In addition, once the trends throughout a typical solution are known, the Fibonacci search windows may be reduced to decrease the computational burden further.

The characteristics of the resulting flight trajectories can be tailored by operations analysis experts by choosing different cost function weightings and providing customized threat models. The difficult task of determining the best set of cost function weightings for changing mission tactics while enroute would require heuristic reasoning supplied by either the pilot or future expert mission management systems.

The limitations discussed in the vertical plane problems result in significant restrictions for practical vertical flight-path generation. An approach for using a modified range that is not time-scale separated has been proposed.[10] This approach was developed for short-haul trajectories without risk, but has potential application to the risk minimization problem.

The horizontal algorithm could be modified to use a combined cost of fuel/time and a composite risk model that includes terrain avoidance and masking data for low-altitude penetration. The point mass airplane model used in this study remains the same for all classes of aircraft. Therefore, trajectories for tactical fighters or autonomous vehicles performing penetration operations could be generated by using the appropriate lift/drag and engine data.

References

[1]Charavarity, A. J. M., "Application of Singular Perturbation Theory to Onboard Aircraft Trajectory Optimization," Boeing Commercial Airplane Company, Seattle, WA, Document D6-51308TN, 1983.

[2]Burrows, J. W., "Fuel-Optimal Aircraft Trajectories with Fixed Arrival Times" *Journal of Guidance, Control, and Dynamics*, Vol. 6, Jan.–Feb. 1983, pp. 14–19.

[3]Mehra, R. K., Washburn, R. B., Sajan, S., and Carroll, J. V., "A Study of the Application of Singular Perturbation Theory," NASA CR-3167, 1979.

[4]Calise, A. J. and Moerder, D. D., "Singular Perturbation Techniques for Real Time Aircraft Trajectory Optimization and Control," NASA CR-3597, 1982.

[5]Chan, Y. K. and Foddy, M., "Real Time Optimal Flight Path Generation by Storage of Massive Data Bases," *Proceedings of the IEEE NEACON 1985*, Institute of Electrical and Electronics Engineers, New York, 1985, pp. 516–521.

[6]Kupferer, R. A. and Halski, D. J., "Tactical Flight Management—Survivable Penetration" *Proceedings of the IEEE NEACON 1984*, Institute of Electrical and Electronics Engineers, New York, 1984, pp. 503–509.

[7]Murphy, W. J., Maroon, W. J., Kupferer, R. A., Halski, D. J., McDonough, W. G., Maschek, T. J. "Tactical Flight Management Exploratory Development Program," McDonnell Aircraft Co., St. Louis, MO, AFWAL-TR-84-3023, April 1984.

[8]Kokotovic, P., Khalil, H. K., and O'Reilly, J., *Singular Perturbation Methods in Control: Analysis and Design*, Academic Press, Orlando, FL, 1986.

[9]Kirk, D. E., *Optimal Control Theory, An Introduction*, Prentice-Hall, Englewood Cliffs, NJ, 1971.

[10]Calise, A. J., "A New Boundary Layer Matching Procedure for Singularly Perturbed Systems," *IEEE Transactions on Automatic Control*, Vol. AC-23, No. 3, June 1978.